Identification of class II ADP-ribosylation factors as cellular factors required for hepatitis C virus replication

Rayan Farhat, Karin Séron, Juliette Ferlin, Lucie Fénéant, Sandrine Belouzard, Lucie Goueslain, Catherine Jackson, Jean Dubuisson, Yves Rouillé

Identification of class II ADP-ribosylation factors as cellular factors required for hepatitis C virus replication

Journal:	*Cellular Microbiology*
Manuscript ID	CMI-15-0214.R2
Manuscript Type:	Research article
Date Submitted by the Author:	n/a
Complete List of Authors:	Farhat, Rayan; Institut Pasteur de Lille, CIIL Séron, Karin; Institut Pasteur de Lille, CIIL Ferlin, Juliette; Institut Pasteur de Lille, Center for Infection & Immunity of Lille Fénéant, Lucie; Institut Pasteur de Lille, CIIL Belouzard, Sandrine; Institut Pasteur de Lille, CIIL Goueslain, Lucie; Institut Pasteur de Lille, CIIL Jackson, Catherine; Institut Jacques Monod, CNRS UMR 7592 Dubuisson, Jean; Institut Pasteur de Lille, CIIL Rouillé, Yves; Institut Pasteur de Lille, Center for Infection & Immunity of Lille
Key Words:	Infection, Membrane, Viruses (phages)

Identification of class II ADP-ribosylation factors as cellular factors required for hepatitis C virus replication

Running title: Class II Arfs and HCV replication

Rayan Farhat[1], Karin Séron[1], Juliette Ferlin[1], Lucie Fénéant[1], Sandrine Belouzard[1], Lucie Goueslain[1,2], Catherine L Jackson[2], Jean Dubuisson[1], Yves Rouillé[1*]

[1]Center for Infection & Immunity of Lille, Inserm U1019, CNRS UMR8204, Institut Pasteur de Lille, Université Lille Nord de France, Lille, France

[2]Institut Jacques Monod, CNRS UMR 7592, Université Paris Diderot, Sorbonne Paris Cité, Paris, France

*Corresponding author. E-mail: yves.rouille@ibl.cnrs.fr; Phone: +33-320-87-10-27; Fax: +33-320-87-12-01.

SUMMARY

GBF1 is a host factor required for hepatitis C virus (HCV) replication. GBF1 functions as a guanine nucleotide exchange factor (GEF) for G-proteins of the Arf family, which regulate membrane dynamics in the early secretory pathway and the metabolism of cytoplasmic lipid droplets. Here we established that the Arf-GEF activity of GBF1 is critical for its function in HCV replication, indicating that it promotes viral replication by activating one or more Arf family members. Arf involvement was confirmed with the use of two dominant-negative Arf1 mutants. However siRNA-mediated depletion of Arf1, Arf3 (class I Arfs), Arf4 or Arf5 (class II Arfs), which potentially interact with GBF1, did not significantly inhibit HCV infection. In contrast, the simultaneous depletion of both Arf4 and Arf5, but not of any other Arf pair, imposed a significant inhibition of HCV infection. Interestingly, the simultaneous depletion of both Arf4 and Arf5 had no impact on the activity of the secretory pathway and induced a compaction of the Golgi and an accumulation of lipid droplets. A similar phenotype of lipid droplet accumulation was also observed when GBF1 was inhibited by brefeldin A. In contrast, the simultaneous depletion of both Arf1 and Arf4 resulted in secretion inhibition and Golgi scattering, two actions reminiscent of GBF1 inhibition. We conclude that GBF1 could regulate different metabolic pathways through the activation of different pairs of Arf proteins.

INTRODUCTION

Hepatitis C virus (HCV) is a positive-sense single-stranded RNA virus of the *Flaviviridae* family. Like other positive RNA viruses, HCV genome is replicated in the cytoplasm of its host cell. During HCV replication, internal membranes of the cell are rearranged and these rearranged membranes likely are replication sites of the viral RNA genome. HCV-induced membrane rearrangements have been named membranous web (Egger *et al.*, 2002). They include double membrane vesicles (DMV) and clusters of small single membrane vesicles of ER origin (Ferraris *et al.*, 2010; Romero-Brey *et al.*, 2012). DMV have also been observed in cells replicating RNA viruses of other families, including *Picornaviridae* (Limpens *et al.*, 2011; Belov *et al.*, 2012) and *Coronaviridae* (Knoops *et al.*, 2008; Ulasli *et al.*, 2010), but not with other viruses of the *Flaviviridae* family (Welsch *et al.*, 2009; Gillespie *et al.*, 2010; Schmeiser *et al.*, 2014).

GBF1, a major regulator of membrane dynamics in the early secretory pathway, has recently emerged as a host factor involved in the replication of several viruses of the *Picornaviridae* (Belov *et al.*, 2008; Lanke *et al.*, 2009), *Coronaviridae* (Verheije *et al.*, 2008), and *Flaviviridae* (Goueslain *et al.*, 2010; Carpp *et al.*, 2014) families. GBF1 is a brefeldin A (BFA)-sensitive guanine nucleotide exchange factor (GEF) for G-proteins of the Arf family (Claude *et al.*, 1999). Arfs recruit and activate a number of effectors, which function in vesicular transport, phospholipid metabolism, actin cytoskeleton regulation and lipid droplet metabolism (Donaldson and Jackson, 2011; Wright *et al.*, 2014). There are 6 Arfs and 16 Arf-like proteins in mammalian cells. Arfs are divided into three classes based on sequence homology. Class I contains Arf1-3, class II contains Arf4 and Arf5, and Arf6 constitutes the sole member of class III (Donaldson and Jackson, 2011; Wright *et al.*, 2014). As an ArfGEF, GBF1 shows selectivity for Arfs of classes I and II (Claude *et al.*, 1999; Szul *et al.*, 2007). GBF1 is a large protein of 206 kDa containing 6

conserved domains (Bui *et al.*, 2009). The GEF activity is catalyzed by the Sec7 domain. Our knowledge of the functions of the other conserved domains of GBF1 is still scarce (Bui *et al.*, 2009; Belov *et al.*, 2010; Bouvet *et al.*, 2013).

The mechanism of action of GBF1 in viral infection is not yet understood. Several lines of evidence indicate that GBF1 is required (Verheije *et al.*, 2008; Goueslain *et al.*, 2010; Carpp *et al.*, 2014) and/or is recruited to viral replication complexes (Verheije *et al.*, 2008; Richards *et al.*, 2014) at the onset of viral replication, but not at later time points. It is generally assumed to function as an ArfGEF activating Arf1, which in turn would recruit the COP-I coatomer, a molecular machinery involved in intracellular transport, which has also been reported to be required for the replication of several positive strand RNA viruses, including HCV (Gazina *et al.*, 2002; Cherry *et al.*, 2006; Tai *et al.*, 2009; Wang *et al.*, 2012). Accordingly, a GBF1-Arf1-COP-I pathway has been proposed to play a role in the replication of HCV (Matto *et al.*, 2011; Zhang *et al.*, 2012; Farhat *et al.*, 2013) and other viruses (Wang *et al.*, 2014). However, a direct functional link between GBF1 activation and COP-I function in HCV replication has not been experimentally demonstrated. For instance, in poliovirus infection, the transient recruitment of GBF1 at replication complexes is not coupled to COP-I recruitment (Richards *et al.*, 2014), suggesting the existence of distinct functions for GBF1 at viral replication complexes and in the secretory pathway of the cell. Indeed, GBF1 may primarily function in poliovirus infection by activating or recruiting other cellular effectors essential for viral replication in an Arf1-independent manner (Belov *et al.*, 2010). During HCV replication, the activation by GBF1 of an Arf1 effector different from COP-I, the phosphatidylinositol 4-kinase III β, has been proposed to be involved in HCV replication (Zhang *et al.*, 2012). However the involvement of this kinase during HCV replication is still controversial (Tai *et al.*, 2009; Vaillancourt *et al.*, 2009; Berger *et al.*, 2009; Borawski *et al.*, 2009; Trotard *et*

al., 2009). Other possibilities for GBF1 function during viral replication include the activation of other members of the Arf family or mechanisms unrelated to Arf activation. For example, the mechanism of action of GBF1 during poliovirus replication has been demonstrated not to depend on its catalytic Sec7 domain and therefore on its GEF activity (Belov *et al.*, 2010). In this study, we investigated the mechanism of action of GBF1 in HCV replication. Our data support a model in which class II Arf proteins mediate GBF1 function.

RESULTS

***Role of the Sec7 domain of GBF1 in HCV infection*.** It has recently been reported that GBF1 but not Arf activation is required for poliovirus replication (Belov *et al.*, 2010), suggesting that GBF1 may have other functions than Arf activation during a viral infection. More specifically, a catalytically inactive GBF1 truncation mutant lacking the Sec7 domain has been reported to be sufficient for rescuing poliovirus replication from BFA inhibition. To investigate if GBF1 could also function in a Sec7-independent manner in HCV replication, we expressed a series of GBF1 truncation mutants (figure 1A) in Huh-7 cells and infected them with HCV in the presence of BFA. We used a dose of 50 ng/ml BFA, which decreases HCV infection about 10 times and has minimal cytotoxic effects in Huh-7 cells during the time scale of the HCV infection assay (Goueslain *et al.*, 2010). We previously showed that BFA has no impact on HCV entry and inhibits the replication step of the HCV life cycle (Goueslain *et al.*, 2010). GBF1 construct expression and HCV infection were probed by immunoblotting at 30 hpi. At this time, only cells initially infected are positive (Afzal *et al.*, 2014), implying that the impact of BFA inhibition of progeny virion release on HCV protein expression is negligible.

BFA treatment had no impact on the expression of GBF1 constructs (figure 1B). In the absence of BFA, similar E1 expression levels were observed with all GBF1 constructs, indicating that none of these constructs had any dominant-negative effect on HCV infection. In the presence of BFA, E1 expression levels were reduced about 10-20 times in untransfected cells or in cells expressing YFP. HCV infection was partially rescued in cells expressing full-length wild-type or M832L BFA-resistant constructs, whereas the E794K inactive mutant was unable to rescue HCV infection in the presence of BFA, as previously reported (Goueslain *et al.*, 2010). Importantly, unlike for poliovirus, all the C-terminal deletion constructs including GBF1(1-710), which lacks a Sec7 domain, were unable to rescue HCV infection in these complementation experiments (figure 1B and C). Therefore, these results support a Sec7-dependent function of GBF1 in HCV infection.

As a control, we also quantified the impact of GBF1 constructs on the secretion of human serum albumin (HSA) by BFA-treated Huh-7 cells. A well-established function of GBF1 is the control of membrane dynamics in the early secretory pathway, and this function relies on Arf activation. Therefore, HSA secretion is a marker of GBF1-mediated Arf activation in these experiments. The treatment of Huh-7 cells with 50 ng/ml BFA decreased albumin secretion in control mock-, or YFP-transfected cells (figure 1D). As expected, wild type and M832L GBF1 constructs partially restored albumin secretion, but none of the other constructs did. These results indicate a similar requirement of GBF1 domains for HCV infection and for Arf activation and are consistent with a requirement of ArfGEF activity to promote HCV infection.

Arf1 dominant negative mutants inhibit HCV infection. Our results with GBF1 truncation mutants suggested that the activation of at least one BFA-sensitive Arf family member is required for HCV infection. We further investigated this question using two

different mutants of Arf1 affecting either GDP exchange (T31N) or GTP hydrolysis (Q71L). When overexpressed, these two constructs act as dominant negative mutants in a protein transport assay and block the intracellular traffic at different steps of the early secretory pathway (Dascher and Balch, 1994). Arf mutants were expressed as EGFP or mCherry fusion proteins in Huh-7 cells and the cells were infected with HCV. The infection was monitored by immunofluorescence (figure 2A) and the percentage of fluorescent cells infected was quantified. As expected, the expression of the T31N mutant, which has a BFA-like effect, strongly inhibited HCV infection (figure 2B). The Q71L mutant, which is locked in the active, GTP-bound form, also strongly inhibited HCV infection, and the wild type Arf1 construct had a moderate impact compared to EGFP and mCherry controls. On the other hand, Arf1 constructs did not have any effect on adenovirus infection, indicating that the effects observed with HCV did not result from any cytotoxic effects of Arf1 constructs. These results confirmed the involvement of an Arf family member in HCV infection.

Role of Arf family members in HCV infection. The results with dominant negative mutants of Arf1 suggest that Arf1 and/or other Arf family members are involved in HCV infection. We used siRNA technology to determine which Arf proteins are specifically involved in HCV infection. Given the BFA sensitivity of HCV infection, we focused our study on class-I and class-II Arfs. Arf1, Arf3, Arf4 and Arf5 (human cells have no Arf2) were targeted with pools of 4 siRNAs, except for Arf1, which was targeted by 2 siRNAs only, because we found that the commercial Arf1 pool contains 2 individual siRNAs also targeting Arf3 (supplementary figure 1). Surprisingly, the depletion of each Arf protein resulted in a moderate (30-35%) inhibition of HCV infection (figure 3A). To assess the extent of siRNA-mediated Arf depletion, we quantified mRNAs by quantitative RT-PCR.

The depletions were specific and reached 87% inhibition for Arf1 and about 95% inhibition for the other Arfs (figure 3B). We also observed an up-regulation of Arf4 expression upon Arf1 and to a lesser extent Arf3 depletion, suggesting the existence of compensatory mechanisms regulating the expression of Arf family members.

Arfs may have overlapping functions, and it has been reported that the depletion of different pairs of Arfs results in specific phenotypes (Volpicelli-Daley *et al.*, 2005). Therefore we considered that a specific pair of Arfs could be involved in HCV infection. For this reason, we also depleted pairs of Arfs. Again, higher levels of Arf4 mRNA were observed upon Arf1+Arf3 depletion or Arf1+Arf5 depletion, confirming the up-regulation of Arf4 in Arf1-depleted cells (figure 3B). Interestingly, HCV infection was decreased down to 17±8% in cells depleted of both Arf4 and Arf5, whereas the depletion of other pairs did not significantly decrease more HCV infection than single Arf depletions (figure 3A). These results indicate a special importance of class-II Arfs in HCV infection.

To rule out off-target effects, Arf4 or Arf5 were expressed in siRNA-treated cells. Arf proteins of murine origin were expressed in Huh-7 cells simultaneously depleted of both Arfs. Immunoblot analysis confirmed Arf5 expression (figure 3C). However, Arf4 expression could not be confirmed due to the lack of reactivity toward murine Arf4 of the antibody. HCV infection was partially restored in Arf4-expressing cells and in Arf5-expressing cells (figure 3D). We also observed a slight decrease of HCV infection in cells transfected with Arf4 in the control condition (figure 3D). The expression of Arf4 or Arf5 in double-depleted cells increased HCV infection up to levels similar to those observed in cells depleted of a single Arf protein (figure 3A). In contrast, no rescue of HCV infection was observed in cells transfected with siRNAs to PI4KA, as expected (figure 3D).

To determine if the replication step of the HCV life cycle is affected by the simultaneous depletion of class-II Arfs, siRNA-transfected Huh-7 cells were electroporated with an in vitro-transcribed recombinant ΔE1E2 JFH1 genomic RNA expressing a *Renilla* luciferase reporter. Measuring luciferase activity over a 72-h time course assessed replication. Luciferase activity was not inhibited at 4h post electroporation, and was reduced about 9 times in cells depleted of Arf4 and Arf5 at 48 and 72 h post electroporation (figure 3E), indicating an inhibition of HCV replication with no impact on the initial translation level of HCV RNA.

We also investigated HCV entry in Huh-7 cells simultaneously depleted of both class II Arfs using HCVpp. As controls, we used VSV-Gpp, which rely on endocytosis and pH-dependent fusion for entry, like HCVpp, and RD114pp, which enter by a pH-independent mechanism. All pseudoparticles were similarly inhibited by the double depletion of Arf4 and Arf5 (supplementary figure 2), indicating a post-fusion inhibition of pseudoparticle entry. Therefore, we cannot conclude on the function of class II Arfs during the entry step of the HCV life cycle.

Class II Arfs are not recruited in HCV replication complexes. The intracellular localization of Arf4 and Arf5 in Huh-7 cells was analyzed by immunofluorescence confocal microscopy. Cells were transfected with expression vectors for Arf4-GFP or Arf5-GFP. Both Arf4-GFP and Arf5-GFP were observed in Golgi-like perinuclear structures together with a diffuse staining of the cytosol and the nucleus (supplementary figure 3), which is consistent with the dual localization of Arf proteins as membrane-associated and soluble proteins. Arf4- and Arf5-positive perinuclear structures were also labeled with an antibody to GM130 (supplementary figure 3A), indicating that they are localized in the cis-Golgi. Interestingly, Arf4 and Arf5 perinuclear structures also colocalized with GBF1 (supplementary figure 3B).

In infected cells, the localization of Arf4-GFP and Arf5-GFP was compared to that of NS3 and NS5A, two markers of HCV replication complexes. We did not observe any major change of Arf4 and Arf5 patterns (supplementary figure 4), except in Arf4-GFP expressing cells, where the Golgi appears less structured. This tendency toward a less compact Golgi was also observed in non-infected cells (supplementary figure 3). Very few levels of colocalization of Arfs and NS3 (supplementary figure 4A) or NS5A (supplementary figure 4B) were observed, indicating that class II Arfs are not permanently recruited to HCV replication complexes.

Impact of Arfs depletion on the secretory pathway. To get insight into a mechanism of action of the pair of class-II Arfs, we analyzed their involvement in the regulation of secretion. Following depletion of different pairs of Arfs, we monitored the secretion of serum albumin and VLDL-associated apolipoprotein E (apoE), two proteins expressed and constitutively secreted by Huh-7 cells. Albumin and apoE secretion were inhibited in cells with reduced levels of both Arf1 and Arf4, but were not affected by the depletion of any other pair of Arfs, including Arf4 and Arf 5 (figure 4A). These results indicate that the simultaneous depletion of class II Arfs has no functional impact on the secretory pathway.

To further examine the impact of their depletion on the secretory pathway, we also investigated the morphology of cellular compartments. We observed a more compact Golgi morphology in cells simultaneously depleted of Arf4 and Arf5 than in control cells using the cis-Golgi marker GM130 (figure 4B). In contrast, the depletion of Arf1 and Arf4 resulted in a fragmentation of the cis-Golgi, as previously reported for HeLa cells (Volpicelli-Daley *et al.*, 2005). A similar scattered Golgi phenotype was observed upon GBF1 depletion (figure 4B) or after a BFA treatment (data not shown). We did not

observe any morphological change in cells depleted of other pairs of Arfs (supplementary figure 5). A compaction of the Golgi complex was also observed in class II Arfs-depleted cells with other markers. In these cells, GBF1 and ERGIC53, two proteins located both in the cis-Golgi and the ERGIC, and TGN46, a marker of the trans-Golgi network, all showed a more compact localization (figure 4B), indicating that the effect is not restricted to the cis-Golgi. Again, the depletion of Arf1 and Arf4 or of GBF1 resulted in a scattered pattern of ERGIC53, GBF1 and TGN46 (figure 4B). No other Arf pair produced similar phenotypes of scattered or compacted patterns with any of the markers (data not shown). These results indicate that the pair of class II Arfs does not contribute to the Golgi scattering effect of GBF1 inhibition.

Impact of class II Arfs depletion on the lipid droplets. In addition to its role as a regulator of the early secretory pathway, GBF1 is also known to regulate lipid droplets (Guo *et al.*, 2008; Beller *et al.*, 2008; Soni *et al.*, 2009), a cellular compartment playing a critical role in the HCV life cycle. Given the lack of effect of class II Arfs on the secretory pathway, we also investigated the morphology of lipid droplets after Arf depletion. Lipid droplets were stained with BODIBY493/503 and the Golgi was also labeled with an antibody to GM130 to verify the effect of Arf4 and Arf5 depletion. In cells simultaneously depleted of Arf4 and Arf5, lipid droplets were larger than in control cells and were packed together at the periphery, often in one extension of the cell, unlike in control cells where smaller lipid droplets were usually scattered throughout the cytoplasm (figure 5A). A similar effect was observed in cells treated for 24 hours with a low dose of BFA (figure 5B), or in cells depleted of GBF1 (data not shown), suggesting that the action of the pair of class II Arfs on lipid droplets is regulated by GBF1. Importantly, the depletion of other Arf pairs did not result in a similar phenotype of accumulation of

enlarged lipid droplets. Lipid droplets were very similar to controls for all depletions except for the pair Arf1 and Arf4, and to some extent the pair Arf3 and Arf4, the depletion of which resulted in a reduced number of enlarged lipid droplets (supplementary figure 5). This result suggests that the pair of class II Arfs could participate in GBF1-mediated regulation of lipid metabolism.

DISCUSSION

In this study we investigated the mechanism of action of GBF1 in HCV infection. Our results suggest that GBF1 functions in HCV infection by activating class II Arfs. This is different from what has been reported for in poliovirus, for which its GEF activity and Arf activation are not required (Belov *et al.*, 2010). A series of GBF1 truncation mutants inactive for regulating the secretory pathway of the cell, including a construct lacking a Sec7 domain, were shown to complement BFA inhibition of poliovirus replication. Here we showed that unlike poliovirus, the same series of GBF1 mutants do not support HCV replication, clearly indicating a difference of action for GBF1 in poliovirus and HCV replication. This requirement for GEF activity was confirmed with the use of Arf1 dominant negative mutants.

The function of GBF1 in HCV replication is also different from its function in membrane traffic, as already suggested by our previous study of BFA resistant cell lines (Farhat *et al.*, 2013). Indeed our results suggest that GBF1 may act by activating different pairs of Arf proteins for the control of HCV replication and of protein secretion. The pair Arf1-Arf4 mediates GBF1 control of the secretory pathway, as already reported (Volpicelli-Daley *et al.*, 2005), whereas the pair Arf4-Arf5 mediates GBF1 function in HCV replication. Recently, Arf4 and Arf5 have also been reported to be involved in dengue virus infection, although for this virus, the function of this pair of Arfs was suggested to

be involved in the assembly step (Kudelko *et al.*, 2012). Interestingly, the depletion of Arf4 was reported to protect cells from BFA toxicity, and this effect also depends on GBF1, Arf1 and Arf5 (Reiling *et al.*, 2013).

Based on siRNA experiments, previous studies, including our own, suggested an involvement of Arf1 in HCV replication (Matto *et al.*, 2011; Zhang *et al.*, 2012; Farhat *et al.*, 2013) that we did not observe in this study. However, in none of these previous studies were the results of siRNA depletions confirmed by re-expressing Arf1, in order to rule out off-target effects. Off-target effects are always a potential pitfall with siRNA experiments, as exemplified by our finding that the commercial siRNA pool targeting Arf1 also inhibits Arf3 expression. Reducing siRNA concentration may help to reduce off-target effects. Using a more efficient transfection agent allowed us to decrease siRNA concentration from 80 nM double transfections previously used down to 20 nM single transfections in this study, with better depletion results on control proteins (data not shown). With these new experimental conditions, Arf1 depletion resulted in a lower inhibition of HCV replication (from about 50% in our previous study (Farhat *et al.*, 2013) down to about 30% inhibition in this study) despite efficient reduction of Arf1 mRNA expression. All single Arf depletions similarly yielded low levels of inhibition of HCV infection, in line with the reported lack of phenotype of single Arf depletion (Volpicelli-Daley *et al.*, 2005). In contrast, we found a stronger inhibition of HCV infection when cells were simultaneously depleted of both Arf4 and Arf5. This finding is not inconsistent with the inhibition of HCV infection by Arf1 dominant negative mutants, because trans dominant phenotypes often result from interactions with regulators (like Arf-GEFs and Arf-GAPs in this case). This suggests that Arf1, Arf4 and Arf5 share common regulators, as also indicated by their common inhibition by BFA.

Specific phenotypes were already reported for different pairs of Arfs (Volpicelli-Daley *et al.*, 2005). In our study, the depletion of Arf4 and Arf5 displayed a BFA-like effect on lipid droplets morphology and on HCV infection that the pair Arf1-Arf4 did not. On the other hand, the depletion of the Arf1-Arf4 pair resulted in a BFA-like inhibition of HSA and ApoE secretion, whereas the depletion of the Arf4-Arf5 pair did not. Cells depleted of Arf1 and Arf4 also displayed a scattered Golgi very similar to what is observed in BFA-treated cells or in cells depleted of GBF1, whereas cells depleted of Arf4 and Arf5 had a more compact Golgi morphology than control cells. This effect is not mimicked by GBF1 inhibition, but is rather reminiscent of cells treated with latrunculin B, an inhibitor of actin polymerization (Valderrama *et al.*, 2001; Dippold *et al.*, 2009). Therefore, the Arf4-Arf5 pair could potentially activate an effector involved in the regulation of the actin cytoskeleton. Alternatively, we can also speculate that this effect could result from an alteration of the metabolism of phosphoinositides, because actin fibers are linked to Golgi membranes by PI4P-interacting protein GOLPH3 (Dippold *et al.*, 2009). Taken together these results suggest that GBF1 fulfills its different cellular functions by activating different pairs of Arfs, which in turn control different aspects of the cellular metabolism.

An intriguing question is how each pair of Arfs controls specific pathways. This appears to be a common feature of G-proteins of the Arf family (Panic *et al.*, 2003; Setty *et al.*, 2003; Volpicelli-Daley *et al.*, 2005; Cohen *et al.*, 2007). A redundancy of action is the simplest explanation, although it is quite difficult to match this model with the diversity of phenotypes observed with the depletion of different pairs of BFA-sensitive Arfs (Volpicelli-Daley *et al.*, 2005). Another model for Arf pair specificity could be the formation of Arf dimers, at the site of interaction with effectors. However, such a kind of interactions has not yet been reported for any Arf effector to our knowledge. It is also

possible that the recruitment or the activation of one Arf would depend on the activation of the other one. Different models compatible with this possibility have been proposed (Cohen *et al.*, 2007; Chun *et al.*, 2008). A cascade of recruitment has been reported for other Arf family members (Panic *et al.*, 2003; Setty *et al.*, 2003; Cohen *et al.*, 2007; Christis and Munro, 2012). This hypothesis would be more compatible if similar phenotypes were observed in cells depleted of either protein and in double depleted cells. However, if the selectivity of the system were not stringent, then it could be compatible with an inhibition only visible in double depleted cells. It would be interesting to determine if such a mode of action actually occurs for Arf1-Arf4 and Arf4-Arf5 pairs.

In conclusion, our results indicate that the role of GBF1 in HCV replication is mediated by its ArfGEF activity and is potentially related to a function of regulation of lipid metabolism, rather than of regulation of the protein secretory pathway. Interestingly, two members of the Arf family, class II Arf4 and Arf5, appear to be of special importance for mediating GBF1 function in HCV replication. Although very little is known about the specific functions of class II Arfs, data from our study and from another group (Takashima *et al.*, 2011) suggest their involvement in the control of lipid metabolism, as evidenced by the abnormal morphology of lipid droplets in cells depleted of both Arf4 and Arf5. However, their mechanism of action is unknown. A role for the drosophila Arf1 homologue Arf79F in controlling the localization of enzymes of the triglyceride metabolism to oleic acid-induced lipid droplets was recently described (Wilfling *et al.*, 2014). It is not yet clear how this might relate to our results with class II Arfs-depleted cells, because the depletion of Arf1 reduced the size of lipid droplets in drosophila cells, instead of increasing it as we observed for simultaneous depletion of both Arf4 and Arf5 in Huh-7 cells. Further studies will be needed to determine the nature of the enzymes or

transporters involved in lipid metabolism that are effectors of Arf4 and Arf5. These proteins may constitute host factors critical for the replication of HCV and potentially other RNA viruses.

EXPERIMENTAL PROCEDURES

Reagents. Dulbecco's modified Eagle's medium (DMEM), phosphate-buffered saline (PBS), goat and fetal calf sera (FCS), BODIBY 493/503 and 4',6-diamidino-2-phenylindole (DAPI) were purchased from Life Technologies. Mowiol 4-88 was from Calbiochem. Protease inhibitors mix (Complete) was from Roche. Other chemicals were from Sigma.

Antibodies. Mouse anti-E1 mAb A4 (Dubuisson *et al.*, 1994) was produced in vitro by using a MiniPerm apparatus (Heraeus) as recommended by the manufacturer. Mouse anti-NS5A mAb 9E10 (Lindenbach *et al.*, 2005) was kindly provided by C. M. Rice (The Rockefeller University). Mouse anti-NS3 mAb 1848 was from Virostat. Rabbit anti-human Arf4 mAb (ab171746) was from Abcam. Mouse anti-Arf5 mAb 1B4 was from Abnova. Sheep anti-TGN46 was from Serotec. Mouse anti-GBF1 and anti-GM130 mAbs were from Transduction Laboratories. Mouse anti-β-tubulin mAb (TUB 2.1) was from Sigma. Mouse anti-HSA (ZMHSA1) was from Invitrogen. Goat anti-HSA (507313) was from Calbiochem. Mouse anti-GFP mAb was from Roche. Alexa 555-conjugated donkey anti-sheep IgG antibody was from Life Technologies. Peroxidase-conjugated goat anti-mouse, and anti-sheep IgG, and cyanine 3-conjugated goat anti-mouse IgG were from Jackson Immunoresearch.

DNA constructs. GBF1 deletion mutants were described previously (Niu *et al.*, 2005; Belov *et al.*, 2010). WT Arf1, Q71L and T31N mutants were kindly provided by B. Hoflack (Technische Universität Dresden, Germany). Arf coding sequence was excised

from pGEM2 plasmids using *Hin*dIII and *Bam*HI and subcloned in pEGFP-N1 (Clonetech) between the same sites to generate Arf1-GFP constructs. To generate Arf1-mCherry constructs, the GFP coding sequence was excised with AgeI and NotI and replaced by mCherry coding sequence PCR-amplified using primers GATCCACCGGTCGCCACCATGGTGAGCAAGGGCGAGGAG and AGAGTCGCGGCCGCTCTACTTGTACAGCTCGTCCATG. Arf4-GFP and Arf5-GFP constructs were as previously described (Chun *et al.*, 2008) and were obtained through Addgene. To generate expression vectors for mouse Arf4 and Arf5 used in rescue experiments, the coding sequences were PCR-amplified from mouse 11-day embryo Marathon-Ready cDNA (Clonetech) using primers CTTAAGCTTCCGCCATGGGCCTCACCATC and GTAGGATCCTTAACGTTTTGAAAGTTCATTTGAC (Arf4) or CTTAAGCTTCCGCCATGGGCCTCACGGTG and GTAGGATCCCTAGCGCTTTGACAGCTCGT (Arf5), and inserted in pCEP4 between HinDIII and BamHI sites. All constructs were verified by sequencing.

Cell culture. Huh-7 (Nakabayashi *et al.*, 1982) cells were grown in Dulbecco's modified Eagle's medium (DMEM), high glucose modification, supplemented with glutamax-I and 10% FCS.

***HCVcc*.** The virus JFH1-CSN6A4 used in this study was based on JFH1, and contained cell culture adaptive mutations (Delgrange *et al.*, 2007) and a reconstituted A4 epitope in E1, as previously described (Goueslain *et al.*, 2010). The plasmid pJFH1-CSN6A4 was linearized with XbaI and treated with the Mung Bean Nuclease (New England Biolabs). In vitro transcripts were generated using the Megascript kit according to the manufacturer's protocol (Ambion). Ten micrograms of in vitro transcribed RNA were delivered into Huh-7 cells by electroporation as described (Kato *et al.*, 2003). For virus production, electroporated cells were passaged 3 days after electroporation and grown

to confluence. The culture medium was collected every day, titrated, aliquoted and stored at -80°C. For infection assays, sub-confluent naïve Huh-7 cells grown in a P24 well were incubated with 50 µl of this virus preparation diluted to 200 µl of medium for 2 hours (M.O.I. ~0.5), and the inoculate was replaced with fresh culture medium. In order to reach near 100% infected cells in experiments with Arf1 mutants, cells were infected with 200 µl of undiluted HCVcc stock with a higher titre, (M.O.I. ~5). In all experiments, infections were scored at 30 hpi.

Adenovirus. A recombinant defective adenovirus expressing a green fluorescent protein (EGFP) was as previously described (Farhat *et al.*, 2013). Cells were infected for 1 hour at 37°C, and fixed for 20 minutes with PFA 3% at 16 hours post-infection.

DNA transfection. Twenty-four hours before transfection, cells were seeded in 24-well clusters to reach ~70% confluence the next day. Cells were transfected with 0.5 µg of plasmid DNA mixed with Trans-IT LT1 reagent following the instructions of the manufacturer (Mirus). Cells transfected with pCEP4-based constructs were co-transfected with pPUR (clonetech) at a 1:20 ratio, and selected for with 5 µg/ml puromycin for 3 days, and cultured with no puromycin for 4 days before siRNA transfection.

RNA interference. RNA interference experiments were carried out with pools of four different synthetic double-stranded siRNAs to the same target (on-target plus smart pool reagents from Dharmacon). Due to an off-target effect with the pool against Arf1 we used a mix of 2 individual siRNAs (J-011580-05-0005 & J-011580-08-0005). The control used in this study was the on-target plus non-targeting siRNA #1 (D-001810-01-20).
For siRNA transfection, 3 µl of lipofectamine RNAi MAX (Life Technologies) were added to 0.5 ml of D-PBS and incubated for 3 min. In a 6-well plate, 2.5 µl of siRNA at 20µM were spotted in the center of a well. In case of double siRNA transfection, 1.25 µl of each

siRNA was used. Then, the diluted transfection reagent was added to the siRNA and the mixture was incubated for 30 min at room temperature. At the end of this incubation, 2.5 10^5 freshly trypsinized cells in a volume of 2 ml of culture medium were added to the transfection mix and the cells were returned to 37°C. Cells were trypsinized 24 h later and seeded on glass cover slips, and analyzed by immunofluorescence 3 or 4 days after siRNA transfection. For quantifying HCV infection, siRNA-treated cells were infected 48 h after trypsinization. Just before infection, extra wells of cells treated with each siRNA were used to extract RNA for quantifying the depletion efficiency. Infected cells were stained with anti-E1 mAb A4 and DAPI at 30 hpi and HCV-infected were counted. At least 5000 cells were counted per experiment for each condition.

***Immunoblotting*.** Cells were rinsed 3 times with cold PBS, and lysed at 4°C for 20 min in a buffer containing 50 mM TrisCl, pH 7.5, 100 mM NaCl, 2 mM EDTA, 1% Triton- X, 0.1% SDS, 1 mM PMSF, and a mix of protease inhibitors (Complete). Insoluble material was removed by centrifugation at 4°C. The protein content was determined by the bicinchoninic acid method as recommended by the manufacturer (Sigma), using bovine serum albumin as the standard. The proteins were then resolved by SDS-PAGE and transferred onto nitrocellulose membranes (Hybond-ECL; Amersham) using a Trans-Blot apparatus (Bio-Rad). Proteins of interest were revealed with specific primary antibodies, followed by species-specific secondary antibodies conjugated to peroxidase. Proteins were visualized using enhanced chemiluminescence (ECL Plus, GE healthcare). The signals were recorded using a LAS 3000 apparatus (Fujifilm). Quantification of unsaturated signals was carried out using the gel quantification function of ImageJ.

Immunofluorescence microscopy. Indirect immunofluorescence labeling was performed as previously described (Rouillé *et al.*, 2006). Lipid droplets were stained with BODIBY 493/503 (0.5 µg/ml; Invitrogen) for 10 min at room temperature. Nuclei

were stained with DAPI. For colocalization experiments, confocal microscopy was carried out with an LSM780 confocal microscope (Zeiss) using a 63X oil immersion objective with a 1.4 numerical aperture. Signals were sequentially collected using single fluorescence excitation and acquisition settings to avoid crossover. Images were processed using Adobe Photoshop software CS4.

BFA rescue experiments. Cells were transfected with GBF1 mutants and then infected with JFH1-CSN6A4 48 h post transfection in the presence of 50 ng/ml of BFA, or the corresponding volume of ethanol (BFA solvent). Cells were lysed at 30 hpi and the expression levels of HCV E1 (A4) were measured by Western blot. The expression level of each mutant with ethanol was set to 100%. The relative expression of HCV E1 of the BFA treated samples was normalized to the ethanol control.

Secretion assays. Sub-confluent cell cultures grown in 12-well plates were incubated for 24 h in 1 ml of complete culture medium. Culture media were collected and centrifuged to remove cells debris. Cells were rinsed with PBS, and lysed for 20 min on ice. The HSA concentration in the supernatants and lysates was determined by ELISA, using human serum albumin (HSA) as a standard, as described (Snooks *et al.*, 2008). Apolipoprotein E was quantified using a commercial ELISA kit from Mabtech. The percentage of secretion was calculated as the percentage of HSA/apoE in the medium divided by the total amount of HSA/apoE in the medium and the lysate.

Replication assay. The construct used for the replication assay (HCVcc-Rluc/ΔE1E2) was as previously described (Goueslain *et al.*, 2010). Huh-7 cells were electroporated with HCVcc-Rluc/ΔE1E2 in vitro transcribed RNA and seeded in 24-well plates. The luciferase activity was measured 4 h, 24 h, 48 h and 72 h post-electroporation using the *Renilla* luciferase assay system kit from Promega.

Quantitative RT–PCR. Total RNA was extracted from siRNA-transfected and control cells using Nucleospin RNA II extraction kit (Macherey-Nagel), which includes a DNAse I treatment. cDNA was obtained from RNA using the High Capacity cDNA Reverse transcription kit (Life Technologies) in a final volume of 20 µl. Quantitative RT–PCR analysis was performed using the Taqman® pre-designed gene expression assay approach (Applied Biosystems), using 1 µl of cDNA and premade probes designed by the manufacturer. The ratio of the mRNA level of each gene to that of large ribosomal protein P0 (RPLP0) endogenous control mRNA was calculated by the ΔΔCt method (Livak and Schmittgen, 2001), and a value of 100 was assigned to control siRNA-transfected cells. Each experiment was performed in triplicate and repeated three times.

HCVpp. The luciferase-based HCV-pseudotyped retroviral particles (HCVpp) infection assay was performed as previously described (Op De Beeck *et al.*, 2004).

ACKNOWLEDGMENTS

This work was supported by grants from the "Agence Nationale de la Recherche sur le SIDA et les hépatites virales" (ANRS) and "Agence Nationale de la Recherche" (ANR) through ERA-NET Infect-ERA program (ANR-13-IFEC-0002-01).

We thank B. Hoflack, C.M. Rice and T. Wakita for providing us with reagents. We are grateful to Sophana Ung for his assistance in the illustrations. Some data were generated with the help of the Imaging Core Facility of the campus Calmette (BICeL).

The authors have no conflict of interest to declare.

REFERENCES

Afzal, M.S., Alsaleh, K., Farhat, R., Belouzard, S., Danneels, A., Descamps, V., *et al.* (2014) Regulation of core expression during the hepatitis C virus life cycle. *Journal of General Virology* **96**:311-321.

Beller, M., Sztalryd, C., Southall, N., Bell, M., Jäckle, H., Auld, D.S., and Oliver, B. (2008) COPI complex is a regulator of lipid homeostasis. *PLoS Biol* **6**: e292.

Belov, G.A., Feng, Q., Nikovics, K., Jackson, C.L., and Ehrenfeld, E. (2008) A critical role of a cellular membrane traffic protein in poliovirus RNA replication. *PLoS Pathog* **4**: e1000216.

Belov, G.A., Kovtunovych, G., Jackson, C.L., and Ehrenfeld, E. (2010) Poliovirus replication requires the N-terminus but not the catalytic Sec7 domain of ArfGEF GBF1. *Cell Microbiol* **12**: 1463–1479.

Belov, G.A., Nair, V., Hansen, B.T., Hoyt, F.H., Fischer, E.R., and Ehrenfeld, E. (2012) Complex dynamic development of poliovirus membranous replication complexes. *J Virol* **86**: 302–312.

Berger, K.L., Cooper, J.D., Heaton, N.S., Yoon, R., Oakland, T.E., Jordan, T.X., *et al.* (2009) Roles for endocytic trafficking and phosphatidylinositol 4-kinase III alpha in hepatitis C virus replication. *Proc Natl Acad Sci USA* **106**: 7577–7582.

Borawski, J., Troke, P., Puyang, X., Gibaja, V., Zhao, S., Mickanin, C., *et al.* (2009) Class III phosphatidylinositol 4-kinase alpha and beta are novel host factor regulators of hepatitis C virus replication. *J Virol* **83**: 10058–10074.

Bouvet, S., Golinelli-Cohen, M.-P., Contremoulins, V., and Jackson, C.L. (2013) Targeting of the Arf-GEF GBF1 to lipid droplets and Golgi membranes. *J Cell Sci* **126**: 4794–4805.

Bui, Q.T., Golinelli-Cohen, M.-P., and Jackson, C.L. (2009) Large Arf1 guanine nucleotide exchange factors: evolution, domain structure, and roles in membrane trafficking and human disease. *Mol Genet Genomics* **282**: 329–350.

Carpp, L.N., Rogers, R.S., Moritz, R.L., and Aitchison, J.D. (2014) Quantitative proteomic analysis of host-virus interactions reveals a role for Golgi brefeldin A resistance factor 1 (GBF1) in dengue infection. *Mol Cell Proteomics* **13**: 2836–2854.

Cherry, S., Kunte, A., Wang, H., Coyne, C., Rawson, R.B., and Perrimon, N. (2006) COPI activity coupled with fatty acid biosynthesis is required for viral replication. *PLoS Pathog* **2**: e102.

Christis, C., and Munro, S. (2012) The small G protein Arl1 directs the trans-Golgi-specific targeting of the Arf1 exchange factors BIG1 and BIG2. *J Cell Biol* **196**: 327–335.

Chun, J., Shapovalova, Z., Dejgaard, S.Y., Presley, J.F., and Melançon, P. (2008) Characterization of class I and II ADP-ribosylation factors (Arfs) in live cells: GDP-bound class II Arfs associate with the ER-Golgi intermediate compartment independently of

GBF1. *Mol Biol Cell* **19**: 3488–3500.

Claude, A., Zhao, B.P., Kuziemsky, C.E., Dahan, S., Berger, S.J., Yan, J.P., *et al.* (1999) GBF1: A novel Golgi-associated BFA-resistant guanine nucleotide exchange factor that displays specificity for ADP-ribosylation factor 5. *J Cell Biol* **146**: 71–84.

Cohen, L.A., Honda, A., Varnai, P., Brown, F.D., Balla, T., and Donaldson, J.G. (2007) Active Arf6 recruits ARNO/cytohesin GEFs to the PM by binding their PH domains. *Mol Biol Cell* **18**: 2244–2253.

Dascher, C., and Balch, W.E. (1994) Dominant inhibitory mutants of ARF1 block endoplasmic reticulum to Golgi transport and trigger disassembly of the Golgi apparatus. *J Biol Chem* **269**: 1437–1448.

Delgrange, D., Pillez, A., Castelain, S., Cocquerel, L., Rouillé, Y., Dubuisson, J., *et al.* (2007) Robust production of infectious viral particles in Huh-7 cells by introducing mutations in hepatitis C virus structural proteins. *J Gen Virol* **88**: 2495–2503.

Dippold, H.C., Ng, M.M., Farber-Katz, S.E., Lee, S.-K., Kerr, M.L., Peterman, M.C., *et al.* (2009) GOLPH3 bridges phosphatidylinositol-4- phosphate and actomyosin to stretch and shape the Golgi to promote budding. *Cell* **139**: 337–351.

Donaldson, J.G., and Jackson, C.L. (2011) ARF family G proteins and their regulators: roles in membrane transport, development and disease. *Nat Rev Mol Cell Biol* **12**: 362–375.

Dubuisson, J., Hsu, H.H., Cheung, R.C., Greenberg, H.B., Russell, D.G., and Rice, C.M. (1994) Formation and intracellular localization of hepatitis C virus envelope glycoprotein complexes expressed by recombinant vaccinia and Sindbis viruses. *J Virol* **68**: 6147–6160.

Egger, D., Wölk, B., Gosert, R., Bianchi, L., Blum, H.E., Moradpour, D., and Bienz, K. (2002) Expression of hepatitis C virus proteins induces distinct membrane alterations including a candidate viral replication complex. *J Virol* **76**: 5974–5984.

Farhat, R., Goueslain, L., Wychowski, C., Belouzard, S., Fénéant, L., Jackson, C.L., *et al.* (2013) Hepatitis C virus replication and Golgi function in brefeldin a-resistant hepatoma-derived cells. *PLoS ONE* **8**: e74491.

Ferraris, P., Blanchard, E., and Roingeard, P. (2010) Ultrastructural and biochemical analyses of hepatitis C virus-associated host cell membranes. *Journal of General Virology* **91**: 2230–2237.

Gazina, E.V., Mackenzie, J.M., Gorrell, R.J., and Anderson, D.A. (2002) Differential requirements for COPI coats in formation of replication complexes among three genera of Picornaviridae. *J Virol* **76**: 11113–11122.

Gillespie, L.K., Hoenen, A., Morgan, G., and Mackenzie, J.M. (2010) The endoplasmic reticulum provides the membrane platform for biogenesis of the flavivirus replication complex. **84**: 10438–10447.

Goueslain, L., Alsaleh, K., Horellou, P., Roingeard, P., Descamps, V., Duverlie, G., *et al.*

(2010) Identification of GBF1 as a cellular factor required for hepatitis C virus RNA replication. *J Virol* **84**: 773–787.

Guo, Y., Walther, T.C., Rao, M., Stuurman, N., Goshima, G., Terayama, K., *et al.* (2008) Functional genomic screen reveals genes involved in lipid-droplet formation and utilization. *Nature* **453**: 657–661.

Kato, T., Date, T., Miyamoto, M., Furusaka, A., Tokushige, K., Mizokami, M., and Wakita, T. (2003) Efficient replication of the genotype 2a hepatitis C virus subgenomic replicon. *Gastroenterology* **125**: 1808–1817.

Knoops, K., Kikkert, M., Worm, S.H.E.V.D., Zevenhoven-Dobbe, J.C., van der Meer, Y., Koster, A.J., *et al.* (2008) SARS-coronavirus replication is supported by a reticulovesicular network of modified endoplasmic reticulum. *PLoS Biol* **6**: e226.

Kudelko, M., Brault, J.-B., Kwok, K., Li, M.Y., Pardigon, N., Peiris, J.S.M., *et al.* (2012) Class II ADP-ribosylation factors are required for efficient secretion of dengue viruses. *Journal of Biological Chemistry* **287**: 767–777.

Lanke, K.H.W., van der Schaar, H.M., Belov, G.A., Feng, Q., Duijsings, D., Jackson, C.L., *et al.* (2009) GBF1, a guanine nucleotide exchange factor for Arf, is crucial for coxsackievirus B3 RNA replication. *J Virol* **83**: 11940–11949.

Limpens, R.W.A.L., van der Schaar, H.M., Kumar, D., Koster, A.J., Snijder, E.J., van Kuppeveld, F.J.M., and Bárcena, M. (2011) The transformation of enterovirus replication structures: a three-dimensional study of single- and double-membrane compartments. *MBio* **2**.

Lindenbach, B.D., Evans, M.J., Syder, A.J., Wölk, B., Tellinghuisen, T.L., Liu, C.C., *et al.* (2005) Complete replication of hepatitis C virus in cell culture. *Science* **309**: 623–626.

Livak, K.J., and Schmittgen, T.D. (2001) Analysis of relative gene expression data using real-time quantitative PCR and the 2(-Delta Delta C(T)) Method. *Methods* **25**: 402–408.

Matto, M., Sklan, E.H., David, N., Melamed-Book, N., Casanova, J.E., Glenn, J.S., and Aroeti, B. (2011) Role for ADP Ribosylation Factor 1 in the Regulation of Hepatitis C Virus Replication. *J Virol* **85**: 946–956.

Nakabayashi, H., Taketa, K., Miyano, K., Yamane, T., and Sato, J. (1982) Growth of human hepatoma cells lines with differentiated functions in chemically defined medium. *Cancer Res* **42**: 3858–3863.

Niu, T.-K., Pfeifer, A.C., Lippincott-Schwartz, J., and Jackson, C.L. (2005) Dynamics of GBF1, a Brefeldin A-sensitive Arf1 exchange factor at the Golgi. *Mol Biol Cell* **16**: 1213–1222.

Op De Beeck, A., Voisset, C., Bartosch, B., Ciczora, Y., Cocquerel, L., Keck, Z., *et al.* (2004) Characterization of functional hepatitis C virus envelope glycoproteins. *J Virol* **78**: 2994–3002.

Panic, B., Whyte, J.R.C., and Munro, S. (2003) The ARF-like GTPases Arl1p and Arl3p act in a pathway that interacts with vesicle-tethering factors at the Golgi apparatus. *Curr*

Biol **13**: 405–410.

Reiling, J.H., Olive, A.J., Sanyal, S., Carette, J.E., Brummelkamp, T.R., Ploegh, H.L., *et al.* (2013) A CREB3-ARF4 signalling pathway mediates the response to Golgi stress and susceptibility to pathogens. *Nat Cell Biol*.

Richards, A.L., Soares-Martins, J.A.P., Riddell, G.T., and Jackson, W.T. (2014) Generation of unique poliovirus RNA replication organelles. *MBio* **5**: e00833–13.

Romero-Brey, I., Merz, A., Chiramel, A., Lee, J.Y., Chlanda, P., Haselman, U., *et al.* (2012) Three-dimensional architecture and biogenesis of membrane structures associated with hepatitis C virus replication. *PLoS Pathog* **8**: e1003056.

Rouillé, Y., Helle, F., Delgrange, D., Roingeard, P., Voisset, C., Blanchard, E., *et al.* (2006) Subcellular localization of hepatitis C virus structural proteins in a cell culture system that efficiently replicates the virus. *J Virol* **80**: 2832–2841.

Schmeiser, S., Mast, J., Thiel, H.-J., and König, M. (2014) Morphogenesis of pestiviruses: new insights from ultrastructural studies of strain Giraffe-1. *J Virol* **88**: 2717–2724.

Setty, S.R.G., Shin, M.E., Yoshino, A., Marks, M.S., and Burd, C.G. (2003) Golgi recruitment of GRIP domain proteins by Arf-like GTPase 1 is regulated by Arf-like GTPase 3. *Curr Biol* **13**: 401–404.

Snooks, M.J., Bhat, P., Mackenzie, J., Counihan, N.A., Vaughan, N., and Anderson, D.A. (2008) Vectorial entry and release of hepatitis A virus in polarized human hepatocytes. *J Virol* **82**: 8733–8742.

Soni, K.G., Mardones, G.A., Sougrat, R., Smirnova, E., Jackson, C.L., and Bonifacino, J.S. (2009) Coatomer-dependent protein delivery to lipid droplets. *J Cell Sci* **122**: 1834–1841.

Szul, T., Grabski, R., Lyons, S., Morohashi, Y., Shestopal, S., Lowe, M., and Sztul, E. (2007) Dissecting the role of the ARF guanine nucleotide exchange factor GBF1 in Golgi biogenesis and protein trafficking. *J Cell Sci* **120**: 3929–3940.

Tai, A.W., Benita, Y., Peng, L.F., Kim, S.-S., Sakamoto, N., Xavier, R.J., and Chung, R.T. (2009) A Functional Genomic Screen Identifies Cellular Cofactors of Hepatitis C Virus Replication. *Cell Host Microbe* **5**: 298–307.

Takashima, K., Saitoh, A., Hirose, S., Nakai, W., Kondo, Y., Takasu, Y., *et al.* (2011) GBF1-Arf-COPI-ArfGAP-mediated Golgi-to-ER transport involved in regulation of lipid homeostasis. *Cell Struct Funct* **36**: 223–235.

Trotard, M., Lepère-Douard, C., Régeard, M., Piquet-Pellorce, C., Lavillette, D., Cosset, F.-L., *et al.* (2009) Kinases required in hepatitis C virus entry and replication highlighted by small interference RNA screening. *The FASEB Journal* **23**: 3780–3789.

Ulasli, M., Verheije, M.H., de Haan, C.A.M., and Reggiori, F. (2010) Qualitative and quantitative ultrastructural analysis of the membrane rearrangements induced by coronavirus. *Cell Microbiol* **12**: 844–861.

Vaillancourt, F.H., Pilote, L., Cartier, M., Lippens, J., Liuzzi, M., Bethell, R.C., *et al.* (2009)

Identification of a lipid kinase as a host factor involved in hepatitis C virus RNA replication. *Virology* **387**: 5–10.

Valderrama, F., Durán, J.M., Babià, T., Barth, H., Renau-Piqueras, J., and Egea, G. (2001) Actin microfilaments facilitate the retrograde transport from the Golgi complex to the endoplasmic reticulum in mammalian cells. *Traffic* **2**: 717–726.

Verheije, M.H., Raaben, M., Mari, M., Lintelo, te, E.G., Reggiori, F., van Kuppeveld, F.J.M., *et al.* (2008) Mouse hepatitis coronavirus RNA replication depends on GBF1-mediated ARF1 activation. *PLoS Pathog* **4**: e1000088.

Volpicelli-Daley, L.A., Li, Y., Zhang, C.-J., and Kahn, R.A. (2005) Isoform-selective effects of the depletion of ADP-ribosylation factors 1-5 on membrane traffic. *Mol Biol Cell* **16**: 4495–4508.

Wang, J., Du, J., and Jin, Q. (2014) Class I ADP-Ribosylation Factors Are Involved in Enterovirus 71 Replication. *PLoS ONE* **9**: e99768.

Wang, J., Wu, Z., and Jin, Q. (2012) COPI is required for enterovirus 71 replication. *PLoS ONE* **7**: e38035.

Welsch, S., Miller, S., Romero-Brey, I., Merz, A., Bleck, C.K.E., Walther, P., *et al.* (2009) Composition and three-dimensional architecture of the dengue virus replication and assembly sites. *Cell Host Microbe* **5**: 365–375.

Wilfling, F., Thiam, A.R., Olarte, M.J., Wang, J., Beck, R., Gould, T.J., *et al.* (2014) Arf1/COPI machinery acts directly on lipid droplets and enables their connection to the ER for protein targeting. *Elife* **3**: e01607–e01607.

Wright, J., Kahn, R.A., and Sztul, E. (2014) Regulating the large Sec7 ARF guanine nucleotide exchange factors: the when, where and how of activation. *Cell Mol Life Sci* **71**: 3419–3438.

Zhang, L., Hong, Z., Lin, W., Shao, R.-X., Goto, K., Hsu, V.W., and Chung, R.T. (2012) ARF1 and GBF1 Generate a PI4P-Enriched Environment Supportive of Hepatitis C Virus Replication. *PLoS ONE* **7**: e32135.

FIGURES LEGENDS

Figure 1. Activity of GBF1 truncation mutants in HCV replication. (A) Schematic representation of GBF1 deletion constructs. Conserved domains are indicated in grey and black. (B) Huh-7 cells were transfected with the indicated constructs, infected 16 h later in the presence or the absence of BFA (50 ng/ml) and lysed 30 hpi. BFA was added during the 2-h infection and was present throughout the experiment. Cell lysates were analyzed by immunoblotting with antibodies to E1 (top), GFP (middle) or tubulin (bottom). (C) Quantification of E1 signals. For each construct, the expression of E1 in the presence of BFA is expressed as a percentage of its expression in the absence of BFA. Values are means ± SD of 3 independent experiments. (D) Transfected Huh-7 cells were incubated for 24 h with 50 ng/ml BFA and the amounts of HSA in cell lysates and culture media were quantified by ELISA. Values are means ± SD of 3 independent experiments and are expressed as percentage of secretion. –BFA, mock-transfected cells incubated in the absence of BFA.

Figure 2. Effect of T31N and Q71L of Arf1 mutants on HCV infection. (A) Huh-7 cells were transfected with plasmids expressing Arf1-GFP (WT), Arf1 T31N-GFP or Arf1 Q71L-GFP, and infected with HCV 16 hours after transfection. The cells were fixed at 30 hpi and infected cells were labeled with an anti-E1 antibody (red). Cells expressing Arf1 constructions were detected by GFP fluorescence (green). Each field is presented in duplicate, with an image corresponding to the infection at the top and the image corresponding to merged signals at the bottom, to facilitate the visualization of the red staining. Arrows indicate cells expressing fluorescent fusion proteins. (B) Huh-7 cells expressing GFP or mCherry (FP) or Arf1 constructs fused to GFP or mCherry were

infected with HCV and the infection was quantified in at least 100 fluorescent cells per experiment for each construct (black series). For mock-transfected cells, the infection in the total population was quantified. A similar analysis was performed with an adenovirus expressing GFP in cells expressing the mCherry constructs (grey series). The results are averages of 3 independent experiments (± SD), * P<0.05, *** P<0.001.

Figure 3. Impact of Arf proteins depletion on HCV replication. (A) Huh-7 cells were transfected with indicated siRNA, infected with HCV or adenovirus at 72 h post transfection, fixed at 30 hpi and processed for detection of infected cells by immunofluorescence. Infection of non-targeting siRNA-treated samples is expressed as 100% (*** P<0.001, 1-way ANOVA). (B) Total RNA was extracted from siRNA-transfected cells at 72 h post transfection, and the indicated mRNAs were quantified by RT-qPCR. mRNA amounts in non-targeting siRNA-treated samples are expressed as 100%. (C) pCEP4, pCEP4-Arf4m or pCEP4-Arf5m (both from mouse) transfected Huh-7 cells were transfected with indicated siRNA and analyzed by immunoblotting at 3 days post transfection using Arf4, Arf5 and tubulin antibodies. Note that the anti-Arf4 antibody does not detect the transfected murine Arf4. (D) pCEP4, pCEP4-Arf4m or pCEP4-Arf5m-transfected Huh-7 cells were transfected with indicated siRNA and infected with HCV 3 days later. Cells were fixed at 30 hpi, labeled with an anti-E1 antibody and the number of infected cells was counted. The number of infected cells in pCEP4/non-targeting siRNA-transfected cells was expressed as 100%. Error bars represent standard error of the means (SEM) from 4 independent experiments (** P<0.01, *** P<0.001, pCEP4-Arf vs pCEP4, 2-way ANOVA). (E) Huh-7 cells were transfected with indicated siRNAs and electroporated 3 days post transfection with a recombinant HCV genome containing a deletion in E1E2 and expressing *Renilla*

luciferase. Samples were harvested for luciferase assay at 4, 24, 48, and 72 h post electroporation. Error bars indicate standard errors of the mean for 3 independent experiments performed in triplicate.

Figure 4. Impact of Arf pair depletion on the secretory pathway. (A) Huh-7 cells transfected with the indicated siRNA were seeded in 12-well plates, and cultured for 24 h. The amounts of human serum albumin (HSA) and of apolipoprotein E (apoE) in the conditioned culture media and in cell lysates were quantified with an ELISA assay and expressed as percentage of secretion. Error bars represent standard deviation of 3 independent experiments performed in duplicate (*** P<0.001, 1-way ANOVA). (B) Huh-7 were transfected with indicated siRNAs and fixed 72 h later. Cells were fixed and processed for immunofluorescent detection of ERGIC53, GBF1, GM130 and TGN46 (white). Nuclei were stained with DAPI (blue). Representative confocal images are shown. Bar, 20 µm.

Figure 5. Impact of Arf4 and Arf5 depletion on lipid droplets. (A) Huh-7 cells were transfected with indicated siRNAs and fixed 72 h later. Cells were fixed and processed for immunofluorescent detection of GM130 (red). Lipid droplets were stained with BODIBY 493/503 (green) and nuclei with DAPI (blue). (B) Huh-7 cells were cultured for 24 h in the presence or the absence of BFA (50 ng/ml), and processed for the detection of lipid droplets and nuclei. Representative confocal images are shown. Bars, 20 µm.

LEGENDS TO THE SUPPLEMENTARY FIGURES

Figure S1. Off-target effect of Arf1 siRNA pool. Huh-7 cells were transfected with indicated siRNA and total RNA was extracted 24 h post transfection. Arf1 and Arf3 mRNAs were quantified by RT-qPCR and mRNA amounts in non-targeting siRNA-treated samples are expressed as 100%.

Figure S2. Impact of class II Arf proteins depletion on HCVpp, VSV-Gpp and RD114pp entry. Huh-7 cells were transfected with indicated siRNA and infected with HCVpp, VSV-Gpp or RD114pp 3 days post transfection. Samples were harvested for luciferase assay at 48 hpi. Error bars indicate standard deviation for 3 independent experiments performed in triplicate.

Figure S3. Immunofluorescence analysis of Arf4 and Arf5 intracellular localization in non infected Huh-7 cells. Huh-7 cells transfected with Arf4-GFP or Arf5-GFP expression plasmids were processed for immunofluorescent detection of GM130 (A) or GBF1 (B). Representative confocal images of transfected cells are shown together with the merge image. Bars, 20 µm.

Figure S4. Immunofluorescence analysis of Arf4 and Arf5 intracellular localization in infected Huh-7 cells. Huh-7 cells infected with HCV and transfected with Arf4-GFP or Arf5-GFP expression plasmids were processed for immunofluorescent detection of NS3 (A) or NS5A (B). Representative confocal images of transfected cells are shown together with the merge image. Bars, 20 µm.

Figure S5. Impact of the depletion of different Arf pairs on lipid droplets. (A) Huh-7 were transfected with indicated siRNAs and fixed 72 h later. Cells were fixed and

processed for immunofluorescent detection of GM130 (red). Lipid droplets were stained with BODIPY 493/503 (green) and nuclei with DAPI (blue). Representative confocal images are shown.

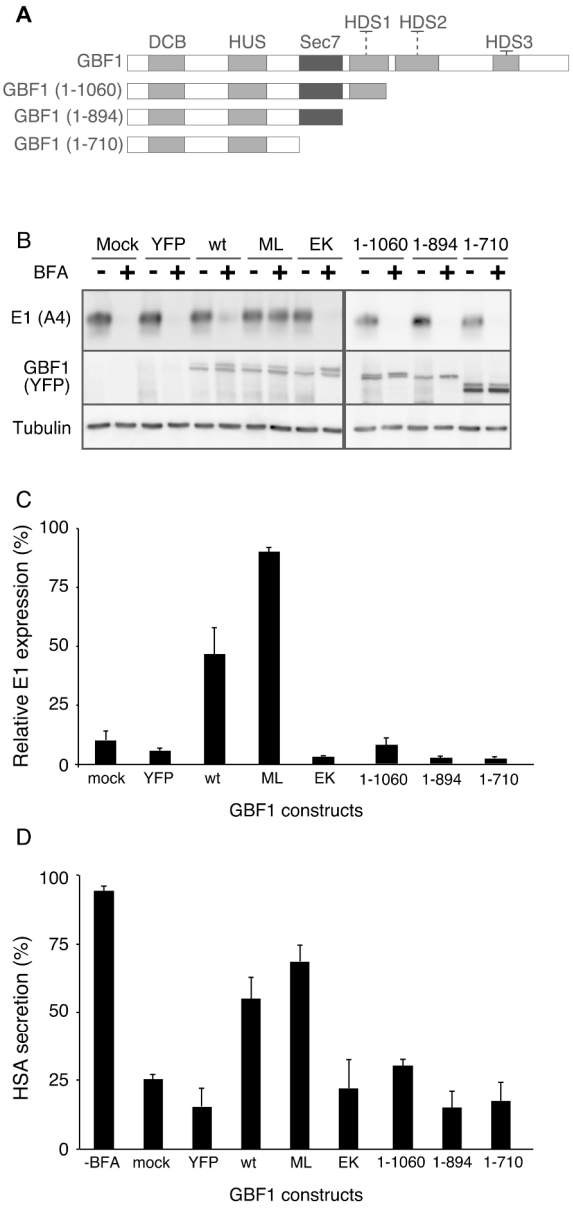

Figure 1. Activity of GBF1 truncation mutants in HCV replication. (A) Schematic representation of GBF1 deletion constructs. Conserved domains are indicated in grey and black. (B) Huh-7 cells were transfected with the indicated constructs, infected 16 h later in the presence or the absence of BFA (50 ng/ml) and lysed 30 hpi. BFA was added during the 2-h infection and was present throughout the experiment. Cell lysates were analyzed by immunoblotting with antibodies to E1 (top), GFP (middle) or tubulin (bottom). (C) Quantification of E1 signals. For each construct, the expression of E1 in the presence of BFA is expressed as a percentage of its expression in the absence of BFA. Values are means ± SD of 3 independent experiments. (D) Transfected Huh-7 cells were incubated for 24 h with 50 ng/ml BFA and the amounts of HSA in cell lysates and culture media were quantified by ELISA. Values are means ± SD of 3 independent experiments and are expressed as percentage of secretion. –BFA, mock-transfected cells incubated in the absence of BFA.
169x356mm (300 x 300 DPI)

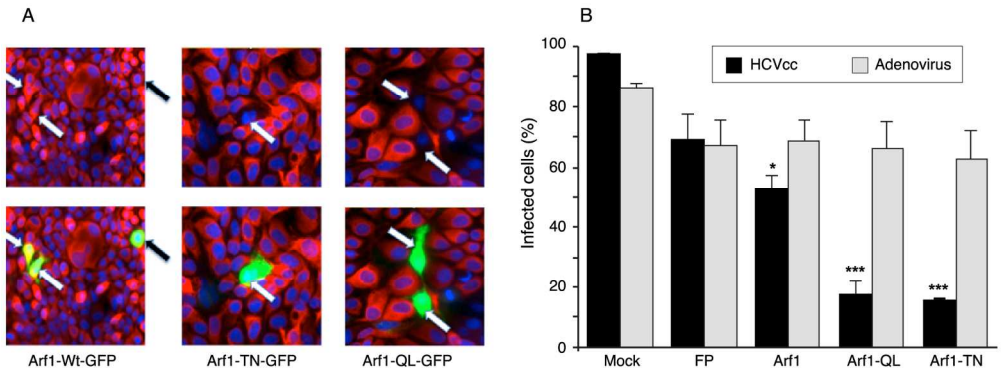

Figure 2. Effect of T31N and Q71L of Arf1 mutants on HCV infection. (A) Huh-7 cells were transfected with plasmids expressing Arf1-GFP (WT), Arf1 T31N-GFP or Arf1 Q71L-GFP, and infected with HCV 16 hours after transfection. The cells were fixed at 30 hpi and infected cells were labeled with an anti-E1 antibody (red). Cells expressing Arf1 constructions were detected by GFP fluorescence (green). Each field is presented in duplicate, with an image corresponding to the infection at the top and the image corresponding to merged signals at the bottom, to facilitate the visualization of the red staining. Arrows indicate cells expressing fluorescent fusion proteins. (B) Huh-7 cells expressing GFP or mCherry (FP) or Arf1 constructs fused to GFP or mCherry were infected with HCV and the infection was quantified in at least 100 fluorescent cells per experiment for each construct (black series). For mock-transfected cells, the infection in the total population was quantified. A similar analysis was performed with an adenovirus expressing GFP in cells expressing the mCherry constructs (grey series). The results are averages of 3 independent experiments (± SD), * $P<0.05$, *** $P<0.001$.
166x61mm (300 x 300 DPI)

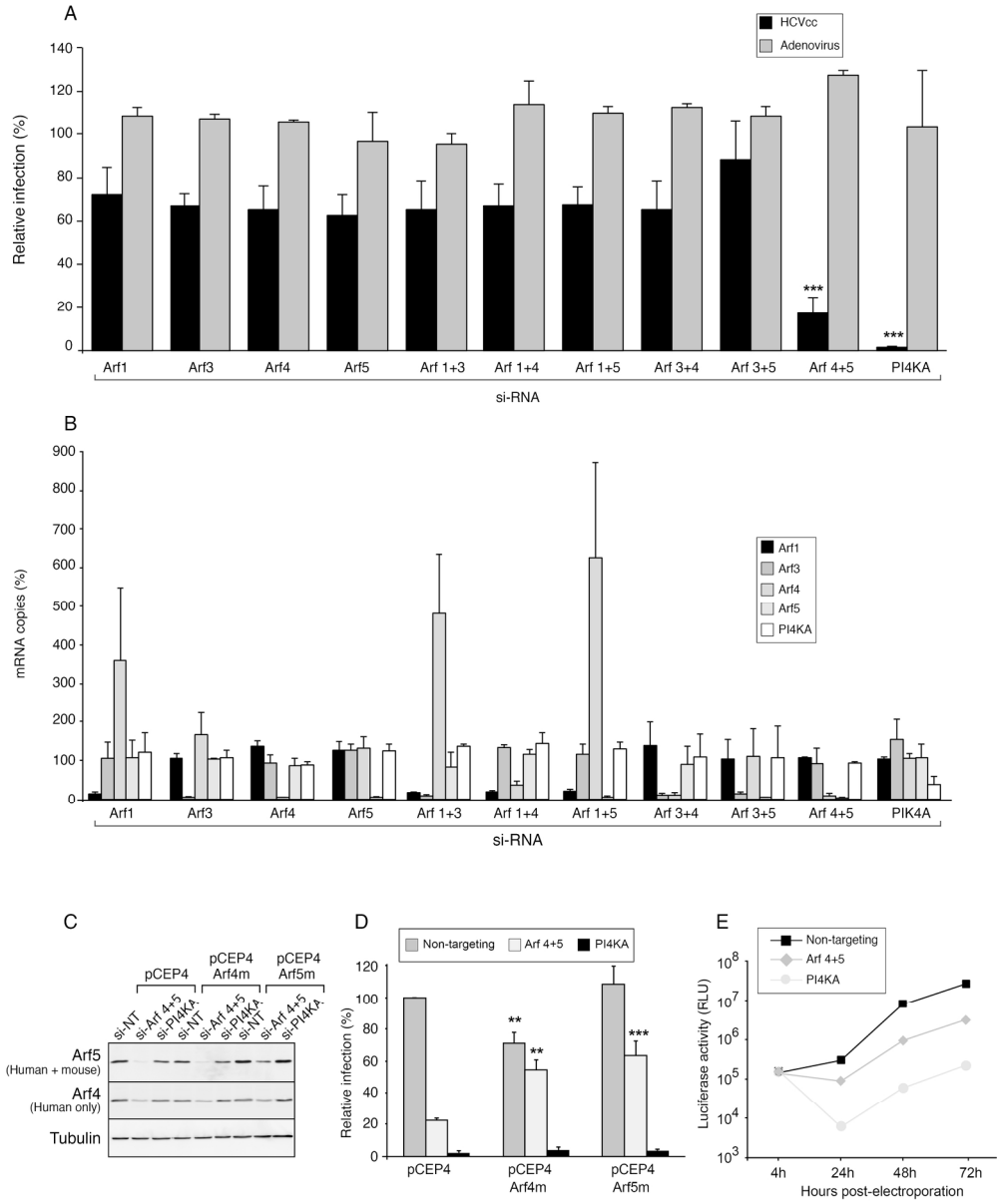

Figure 3. Impact of Arf proteins depletion on HCV replication. (A) Huh-7 cells were transfected with indicated siRNA, infected with HCV or adenovirus at 72 h post transfection, fixed at 30 hpi and processed for detection of infected cells by immunofluorescence. Infection of non-targeting siRNA-treated samples is expressed as 100% (*** P<0.001, 1-way ANOVA). (B) Total RNA was extracted from siRNA-transfected cells at 72 h post transfection, and the indicated mRNAs were quantified by RT-qPCR. mRNA amounts in non-targeting siRNA-treated samples are expressed as 100%. (C) pCEP4, pCEP4-Arf4m or pCEP4-Arf5m (both from mouse) transfected Huh-7 cells were transfected with indicated siRNA and analyzed by immunoblotting at 3 days post transfection using Arf4, Arf5 and tubulin antibodies. Note that the anti-Arf4 antibody does not detect the transfected murine Arf4. (D) pCEP4, pCEP4-Arf4m or pCEP4-Arf5m-transfected Huh-7 cells were transfected with indicated siRNA and infected with HCV 3 days later. Cells were fixed at 30 hpi, labeled with an anti-E1 antibody and the number of infected cells was counted. The number of infected cells in pCEP4/non-targeting siRNA-transfected cells was expressed as 100%. Error bars represent standard error of the means (SEM) from 4 independent experiments (** P<0.01, *** P<0.001, pCEP4-Arf vs pCEP4, 2-way

ANOVA). (E) Huh-7 cells were transfected with indicated siRNAs and electroporated 3 days post transfection with a recombinant HCV genome containing a deletion in E1E2 and expressing Renilla luciferase. Samples were harvested for luciferase assay at 4, 24, 48, and 72 h post electroporation. Error bars indicate standard errors of the mean for 3 independent experiments performed in triplicate.
192x231mm (300 x 300 DPI)

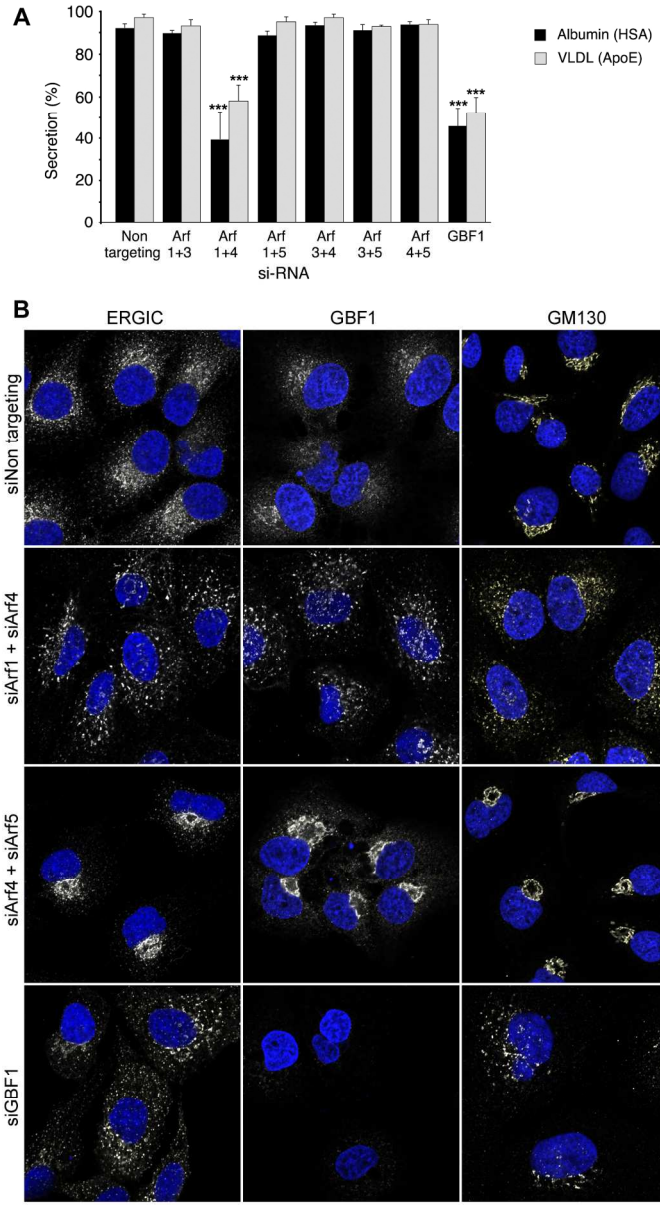

Figure 4. Impact of Arf pair depletion on the secretory pathway. (A) Huh-7 cells transfected with the indicated siRNA were seeded in 12-well plates, and cultured for 24 h. The amounts of human serum albumin (HSA) and of apolipoprotein E (apoE) in the conditioned culture media and in cell lysates were quantified with an ELISA assay and expressed as percentage of secretion. Error bars represent standard deviation of 3 independent experiments performed in duplicate (*** $P<0.001$, 1-way ANOVA). (B) Huh-7 were transfected with indicated siRNAs and fixed 72 h later. Cells were fixed and processed for immunofluorescent detection of ERGIC53, GBF1, GM130 and TGN46 (white). Nuclei were stained with DAPI (blue). Representative confocal images are shown. Bar, 20 µm.
157x211mm (300 x 300 DPI)

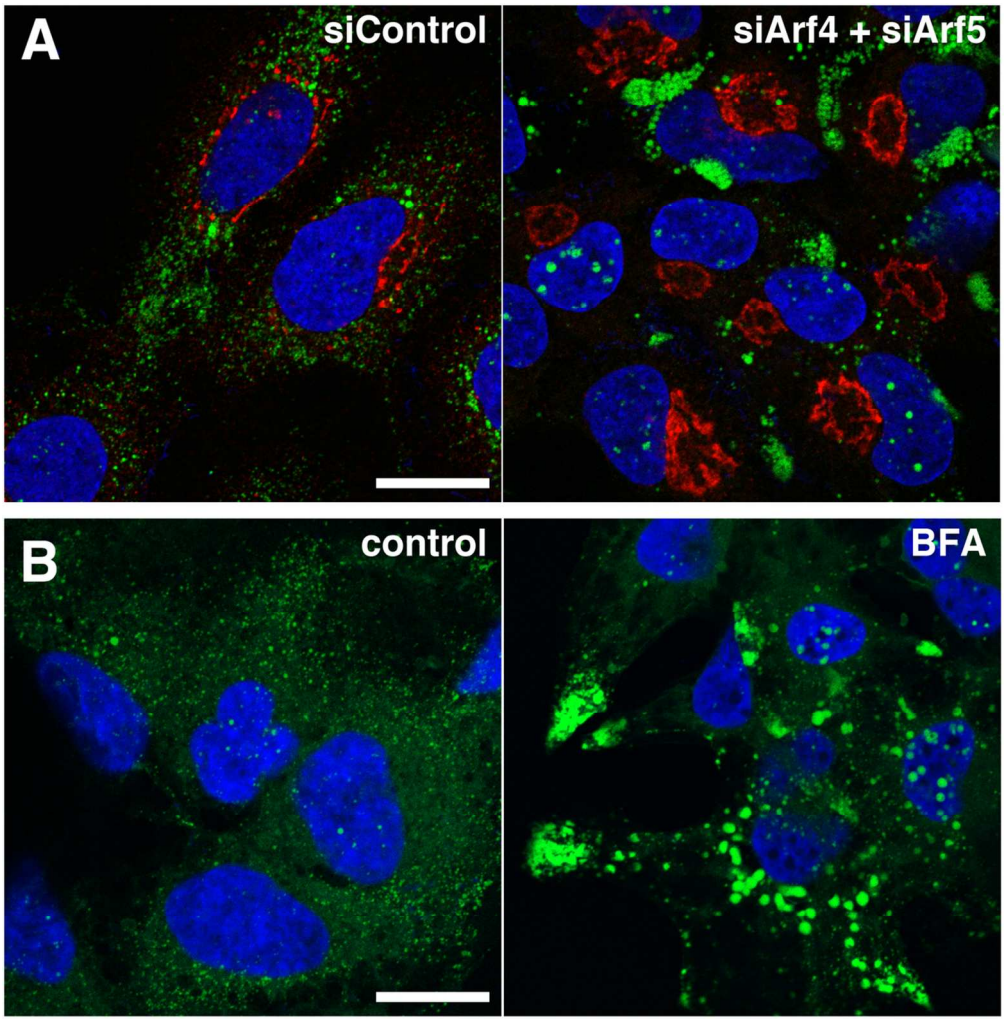

Figure 5. Impact of Arf4 and Arf5 depletion on lipid droplets. (A) Huh-7 cells were transfected with indicated siRNAs and fixed 72 h later. Cells were fixed and processed for immunofluorescent detection of GM130 (red). Lipid droplets were stained with BODIBY 493/503 (green) and nuclei with DAPI (blue). (B) Huh-7 cells were cultured for 24 h in the presence or the absence of BFA (50 ng/ml), and processed for the detection of lipid droplets and nuclei. Representative confocal images are shown. Bars, 20 µm.
111x113mm (300 x 300 DPI)